

ORIGINAL RESEARCH

Open Access



# Diagnostic models for fever of unknown origin based on $^{18}\text{F}$ -FDG PET/CT: a prospective study in China

Jia Chen<sup>1</sup>, MingYou Xing<sup>1</sup>, Dong Xu<sup>1</sup>, NaNa Xie<sup>1</sup>, WenCong Zhang<sup>1</sup>, QiuRong Ruan<sup>2</sup> and JianXin Song<sup>1\*</sup>

## Abstract

**Background:** This study aims to analyze the  $^{18}\text{F}$ -fluorodeoxyglucose positron emission tomography/computed tomography ( $^{18}\text{F}$ -FDG PET/CT) characteristics of different causes of fever of unknown origin (FUO) and identify independent predictors to develop a suitable diagnostic model for distinguishing between these causes. A total of 524 patients with classical FUO who underwent standard diagnostic procedures and PET/CT were prospectively studied. The diagnostic performance of PET/CT imaging was analyzed, and relevant clinical parameters that could improve diagnostic efficacy were identified. The model was established using the data of 369 patients and the other 155 patients comprised the validation cohort for verifying the diagnostic performance of the model.

**Results:** The metabolic characteristics of the “hottest” lesion, the spleen, bone marrow, and lymph nodes varied for various causes. PET/CT combined with clinical parameters achieved better discrimination in the differential diagnosis of FUO. The etiological diagnostic models included the following factors: multisite metabolic characteristics, blood cell counts, inflammatory indicators (erythrocyte sedimentation rate, C-reactive protein, serum ferritin, and lactate dehydrogenase), immunological indicators (interferon gamma release assay, antinuclear antibody, and anti-neutrophil cytoplasm antibody), specific signs (weight loss, rash, and splenomegaly), and age. In the testing cohort, the AUCs of the infection prediction model, the malignancy diagnostic model, and the noninfectious inflammatory disease prediction model were 0.89 (95% CI 0.86–0.92), 0.94 (95% CI 0.92–0.97), and 0.95 (95% CI 0.93–0.97), respectively. The corresponding AUCs for the validation cohort were 0.88 (95% CI 0.82–0.93), 0.93 (95% CI 0.89–0.98), and 0.95 (95% CI 0.92–0.99), respectively.

**Conclusions:**  $^{18}\text{F}$ -FDG PET/CT has a certain level of sensitivity and accuracy in diagnosing FUO, which can be further improved by combining it with clinical parameters. Diagnostic models based on PET/CT show excellent performance and can be used as reliable tools to discriminate the cause of FUO.

**Trial registration** This study (a two-step method apparently improved the physicians' level of diagnosis decision-making for adult patients with FUO) was registered on the website <http://www.clinical-trials.gov> on January 14, 2014, with registration number NCT02035670.

**Keywords:** FUO,  $^{18}\text{F}$ -FDG PET/CT, Clinical parameters, Diagnostic model

\*Correspondence: [songsingsjx@sina.com](mailto:songsingsjx@sina.com)

<sup>1</sup> Department of Infectious Diseases, Tongji Hospital, Tongji Medical College, Huazhong University of Science and Technology, 1095 Jiefang Avenue, Wuhan 430030, China

Full list of author information is available at the end of the article

## Introduction

Fever of unknown origin (FUO) was originally described by Petersdorf and Beeson as a temperature repeatedly higher than 38.3 °C for at least 3 weeks with no ascertainable cause after a week of hospitalization and investigation [1]. FUO remains a substantial challenge

for clinicians due to its inclusion of approximately 200 potential causes in four categories: infections, noninfectious inflammatory diseases (NIIDs), malignancies, and miscellaneous causes [2–6]. The pathophysiology, treatment, and prognosis of these categories differ markedly [7]. Early identification of the underlying category is important to optimize treatment strategies for patients with FUO [8–10]. Currently,  $^{18}\text{F}$ -fluorodeoxyglucose positron emission tomography/computed tomography ( $^{18}\text{F}$ -FDG PET/CT) is considered one of the most promising diagnostic tools for FUO [11–29].

Previous studies have mainly been small case series (between 24 and 376 cases) and retrospective studies [11–21]. The application of PET/CT in etiological classification of FUO was not sufficient. Although PET/CT can provide some diagnostic clues, it is difficult to directly provide a definitive etiological diagnosis of FUO. Therefore, we conducted a study in a Chinese population to explore the PET/CT characteristics for different causes of FUO and further evaluate the clinical significance of PET/CT in the diagnosis of FUO. Specifically, the purpose of this study was to identify the most suitable model for diagnosing patients with FUO based on PET/CT imaging.

## Methods

This study aims to analyze the PET/CT characteristics of different causes of FUO and identify independent predictors to develop a suitable diagnostic model for distinguishing between these causes.

### Patients and standard diagnostic work-up

This prospective study recruited patients older than 14 years of age with a diagnosis of classical FUO who were hospitalized at Tongji Hospital in Wuhan, Hubei Province, China, from January 2016 to July 2021, finally including 369 patients admitted to the Department of Infectious Diseases and 155 patients admitted to other departments (i.e., the Department of Hematology, the Department of Rheumatology, and the Department of Pulmonary and Critical Care Medicine). All enrolled patients underwent a defined standard diagnostic work-up and  $^{18}\text{F}$ -FDG PET/CT scans when there were no potential diagnostic clues (PDCs). Classical FUO was defined as follows: (1) an illness of more than 3 weeks in duration, (2) temperature exceeding  $38.3\text{ }^{\circ}\text{C}$  on more than three occasions, and (3) an uncertain diagnosis despite appropriate investigation, with at least three outpatient visits or at least 3 days of hospitalization [5]. The exclusion criteria were as follows: (1) nosocomial FUO, (2) immunodeficiency-associated FUO, and (3) travel-associated FUO. All enrolled patients were followed up within 6 months via telephone. This study

on FUO was registered on the website <http://www.clinical-trials.gov> on January 14, 2014, with registration number NCT02035670. The research protocol was reviewed and approved by the Huazhong University of Science and Technology Clinical Trial Ethics Committee ([2014] EC-No. 16). Written informed consent was obtained from all participants.

Standard diagnostic procedures included the first step: a thorough patient history questionnaire (a written medical history questionnaire from a previous study), careful physical examination, and obligatory investigation (e.g., hemoglobin, platelet count, leukocyte count and differentiation, creatine, total protein, protein electrophoresis, aspartate aminotransferase, alanine aminotransferase, erythrocyte sedimentation rate [ESR], C-reactive protein, lactate dehydrogenase [LDH], serum ferritin [SF], procalcitonin, antinuclear antibody [ANA], anti-neutrophil cytoplasm antibody [ANCA], interferon gamma release assay [IGRA], blood culture [ $n=3$ ], urine culture, chest CT, and ultrasound) [15, 30]. When PDCs were absent, PET/CT was performed, and further confirmatory procedures (e.g., biopsy, culture, response to diagnostic therapy) were selected based on the results. Changes in relevant blood indicators were monitored, and their dynamic processes were recorded. The final clinical diagnosis of each patient was established by the study team based on the results of all standard procedures, including laboratory, radiological, histopathological findings, and clinical course, according to relevant disease diagnosis guidelines. It was further confirmed by follow-up for 6 months. The causes were divided into five categories: infection, NIID, malignancy, miscellaneous cause, and unknown cause.

### PET/CT scans

The PET/CT scanner used in this study was a Discovery PET/CT 690 (GE Healthcare). PET/CT scans were acquired using standard techniques based on the guidelines issued by the Chinese Society of Nuclear Medicine (fasting for at least 6 h, blood glucose levels below  $11.1\text{ mmol/l}$ , and imaging performed 1 h after injection of  $2.96\text{--}4.44\text{ MBq/kg}$  of FDG) [31]. Emission and transmission images of the area between the proximal femur and the base of the skull were obtained. Attenuation correction and image reconstruction were carried out with an iterative method. Lesion FDG uptake was quantitatively evaluated by using the maximum standardized uptake value (SUV<sub>max</sub>). PET/CT images were independently evaluated by two experienced nuclear medicine physicians who were blinded to the detailed clinical data. Any disagreements were resolved by consensus.

### Statistical analysis

Statistical analysis was performed using SPSS Statistics 26.0 Software (IBM, Chicago). Data are presented as the mean  $\pm$  SD, median [IQR], or frequencies (percentage), when appropriate. Comparisons of continuous variables between groups were performed with Student's *t* test or the Mann–Whitney U test depending on the data distribution. Categorical variables were compared between groups using the  $\chi^2$  or Fisher's exact test according to the theoretical frequency. Two-sided *p* values  $< 0.05$  were considered to indicate significance.

Univariate analysis was used to screen potential diagnostic indicators. All candidate variables with *p* values  $< 0.20$  in the univariate analysis were included in a multivariate analysis to identify the indexes eligible for inclusion in the model. The significance level was set at *p*  $< 0.05$  in the multivariate analysis. The results of the multivariate analysis are presented as odds ratios (ORs) and 95% confidence intervals (CIs). The area under the receiver operating characteristic curve (AUC) was used to evaluate the performance of the prediction model.

## Results

### Patients' characteristics and diagnoses

Overall, 524 FUO patients were enrolled in this study, including 285 males (285/524, 54.4%), with a median age of 49 years [32–61 years]. The duration of fever ranged

from 21 to 732 days, with a median of 37 days. Infectious diseases, tumors, NIIDs, and miscellaneous causes were reported in 223, 121, 109, and 22 patients, respectively, while the remaining 49 patients were undiagnosed after 6 months of follow-up. The final etiological classifications and clinical diagnoses are listed in Additional file 1: Table S1. Tuberculosis accounted for the largest proportion of infections (52/223, 23.3%), while lymphoma was the most common tumor (77/121, 63.6%). Half of the NIID patients (56/109, 51.4%) had adult-onset Still's disease. There was no significant difference in etiological composition or patient characteristics between patients from the Department of Infectious Diseases and those from other departments (Table 1).

### PET/CT characteristics and performance in diagnosing FUO

PET/CT examinations showed positive findings in 477 (477/524, 91.0%) patients (diffuse or focal high uptake of FDG in various organs and tissues) (Table 2). All patients with neoplasms had positive results. The locations of the lesions with the highest FDG uptake in different etiologies were listed in Additional file 1: Table S2. Lymph nodes and bone marrow were the most common sites with the highest uptake among all etiologies. Hyperenhancement of the nasopharynx was common in tumors, and hyperenhancement of the bone or joint was common in inflammation. The SUVmax for

**Table 1** Characteristics of individuals and etiological composition between patients from different departments

	Patients from the department of infectious diseases (n = 369)	Patients from other departments (n = 155)	<i>p</i> value
Sex male	193 (52.3)	92 (59.4)	0.139
Age (years)	48 [32–60]	50 [32–62]	0.315
Duration of fever (days)	37 [28–57]	38 [28–65]	0.564
Infection	157 (42.5)	66 (42.6)	0.969
Malignancy	85 (23.0)	36 (23.2)	
NIID	76 (20.6)	33 (21.3)	
Miscellaneous cause	17 (4.6)	5 (3.2)	
Unknown cause	34 (9.2)	15 (9.7)	

N (%), median [IQR]

NIID noninfectious inflammatory disease

**Table 2** Positive findings and SUVmax of PET/CT for patients with FUO

PET/CT findings	Infection	Malignancy	NIID	Miscellaneous	Unknown	<i>p</i> value
Positive	193 (86.5) <sup>a</sup>	121 (100) <sup>b</sup>	99 (90.8) <sup>a</sup>	22 (100) <sup>a, b</sup>	42 (85.7) <sup>a</sup>	0.000
SUVmax	5.4 [4.0, 9.0] <sup>a, c</sup>	10.8 [6.7, 16.4] <sup>b</sup>	5.1 [3.9, 6.5] <sup>a</sup>	8.3 [5.5, 12.3] <sup>b, c</sup>	7.8 [5.8, 9.1] <sup>b</sup>	0.000

N (%), median [IQR]

SUVmax the maximum standardized uptake value; PET/CT positron emission tomography/computed tomography; FUO fever of unknown origin; NIID noninfectious inflammatory disease

<sup>a, b, c</sup> Pairwise comparison between subgroups, *p* values  $< 0.05$

the “hottest” lesions was significantly higher in patients with malignancy than that in patients with infections and NIIDs ( $p < 0.05$ ). The AUC of SUVmax was 0.79 (95% CI 0.74–0.84) in diagnosing cancer, 0.65 (95% CI 0.60–0.70) in diagnosing infection, and 0.64 (95% CI 0.59–0.69) in diagnosing NIID (Fig. 1).

Many patients showed FDG avidity in multiple sites, most commonly in the spleen, bone marrow, and lymph nodes (Table 3). The metabolic characteristics of the spleen, bone marrow, and peripheral lymph nodes (cervical, axillary, and inguinal lymph nodes) were consistent. Specifically, the increased FDG uptake was more common, and the corresponding SUVmax was higher

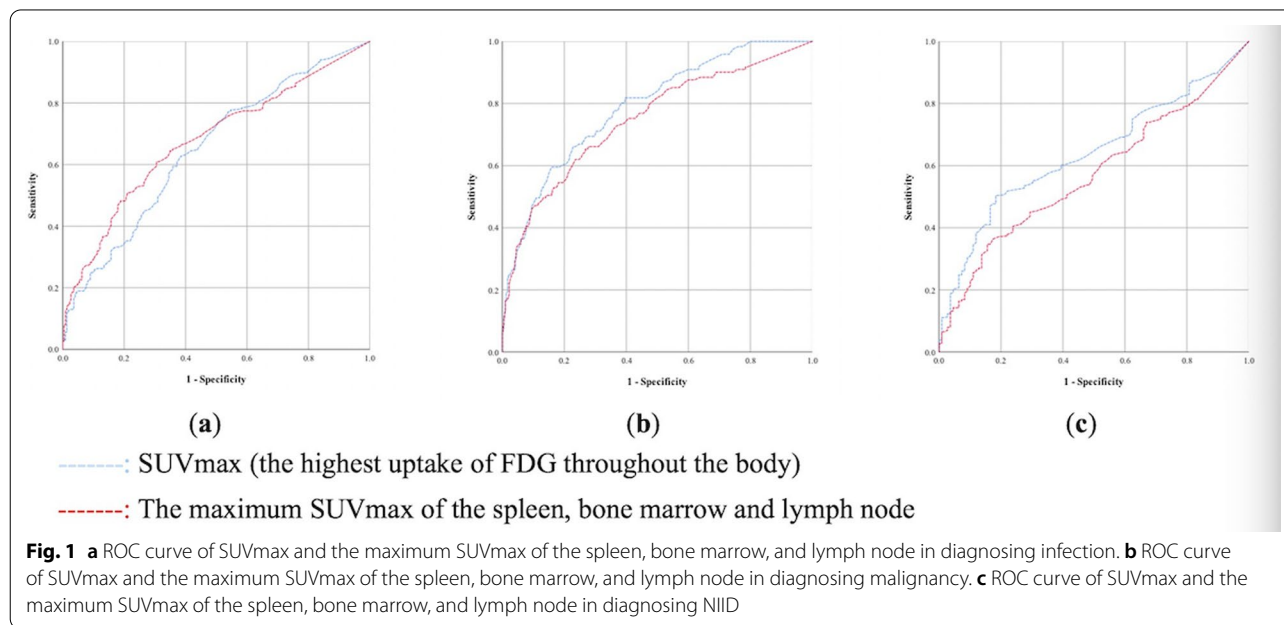


**Table 3** Increased FDG uptake in the spleen, bone marrow, and lymph nodes for patients with FUO

Location	Characteristics	Infection	Malignancy	NIID	Miscellaneous	Unknown	p value
Spleen	Hypermetabolism	50 (22.4) <sup>a</sup>	64 (52.9) <sup>b</sup>	50 (45.9) <sup>b</sup>	5 (22.7)	27 (55.1)	0.000
	SUVmax	3.6 [3.0, 4.3] <sup>a</sup>	5.2 [3.6, 7.8] <sup>b</sup>	3.9 [3.3, 5.0] <sup>a</sup>	3.0 [2.7, 4.4]	4.3 [3.4, 5.5]	0.000
bone marrow	Hypermetabolism	48 (21.5) <sup>a</sup>	53 (43.8) <sup>b</sup>	41 (37.6) <sup>b</sup>	4 (18.2)	18 (36.7)	0.000
	SUVmax	4.4 [3.5, 5.1] <sup>a</sup>	6.6 [4.4, 10.2] <sup>b</sup>	4.4 [3.7, 5.4] <sup>a</sup>	5.5 [4.2, 6.8]	4.6 [3.7, 5.7]	0.000
Lymph node	Hypermetabolism	149 (66.8) <sup>a</sup>	95 (78.5) <sup>a</sup>	74 (67.9) <sup>a</sup>	18 (81.8)	33 (67.3)	0.129
	SUVmax	4.0 [2.9, 6.4] <sup>a</sup>	9.1 [4.4, 14.3] <sup>b</sup>	4.3 [2.8, 6.4] <sup>a</sup>	8.7 [4.6, 12.3]	7.4 [5.6, 9.0]	0.000
Cervical LN	Hypermetabolism	83 (37.2) <sup>a</sup>	66 (54.5) <sup>b</sup>	57 (52.3) <sup>b</sup>	16 (72.7)	26 (53.1)	0.001
	SUVmax	3.5 [2.4, 5.6] <sup>a</sup>	5.6 [3.0, 13.5] <sup>b</sup>	3.8 [2.5, 5.3] <sup>a</sup>	8.2 [4.2, 12.6]	6.0 [4.0, 8.0]	0.000
Axillary LN	Hypermetabolism	41 (18.4) <sup>a</sup>	40 (33.1) <sup>b</sup>	48 (44.0) <sup>b</sup>	8 (36.4)	23 (46.9)	0.000
	SUVmax	2.7 [1.9, 4.3] <sup>a</sup>	5.3 [2.4, 12.4] <sup>b</sup>	3.3 [1.9, 5.1] <sup>a</sup>	7.7 [4.1, 10.5]	6.5 [2.9, 8.1]	0.000
Inguinal LN	Hypermetabolism	19 (8.5) <sup>a</sup>	28 (23.1) <sup>b</sup>	26 (23.9) <sup>b</sup>	7 (31.8)	11 (22.4)	0.000
	SUVmax	2.9 [1.7, 3.6] <sup>a</sup>	5.0 [2.3, 14.2] <sup>b</sup>	2.9 [1.9, 4.4] <sup>a</sup>	2.9 [1.4, 4.8]	3.1 [1.8, 5.4]	0.021
Mediastinal LN	Hypermetabolism	95 (42.6) <sup>a</sup>	58 (47.9) <sup>a</sup>	43 (39.4) <sup>a</sup>	4 (18.2)	18 (36.7)	0.101
	SUVmax	3.9 [2.9, 5.2] <sup>a</sup>	5.8 [3.2, 14.0] <sup>b</sup>	4.2 [3.0, 6.7] <sup>a, b</sup>	5.0 [3.5, 6.7]	6.0 [3.5, 7.6]	0.008
Retroperitoneal LN	Hypermetabolism	53 (23.8) <sup>a</sup>	66 (54.5) <sup>b</sup>	33 (30.3) <sup>a</sup>	10 (45.5)	23 (46.9)	0.000
	SUVmax	3.7 [2.6, 6.8] <sup>a</sup>	9.7 [5.2, 14.6] <sup>b</sup>	4.3 [3.3, 6.0] <sup>a</sup>	7.4 [5.2, 9.0]	5.2 [3.6, 7.7]	0.000

N (%), median [IQR]

FDG fluorodeoxyglucose; FUO fever of unknown origin; NIID noninfectious inflammatory disease; SUVmax the maximum standardized uptake value; LN lymph node

<sup>a, b</sup> Pairwise comparison between subgroups, p values < 0.05

in patients with tumors, while related indexes were significantly decreased in patients with infectious diseases ( $p < 0.05$ ). Patients with NIIDs presented with high rates of hypermetabolism, similar to those with malignancies, but a lower corresponding SUVmax than patients with malignancies ( $p < 0.05$ ). The metabolic characteristics of the central lymph nodes were different. The incidence of increased FDG avidity in the retroperitoneal lymph nodes in NIID patients was lower than that in patients with tumors ( $p < 0.05$ ). There was no significant difference in the proportion of mediastinal lymph node hypermetabolism among the groups. Further analysis confirmed that the metabolic characteristics of the spleen, bone marrow and lymph nodes performed modestly in categorizing FOU etiology into infection, malignancy, and NIID, and the AUCs of the above indicators were mostly less than 0.7 (Additional file 1: Fig. S1). The maximum SUVmax of the spleen, bone marrow, and lymph node yielded an AUC of 0.75 (95% CI 0.69–0.80) in diagnosing cancer, 0.68 (95% CI 0.63–0.72) in diagnosing infection, and 0.57 (95% CI 0.52–0.63) in diagnosing NIID (Fig. 1).

### Diagnostic model construction

Due to the small number of patients with no diagnosis and miscellaneous diseases, the lack of commonality among those diseases, and the desire to use all the data to meet real-life settings, three categories were adopted: infectious disease and noninfectious disease; malignant disease and nonmalignant disease; and NIID and non-NIID. A clinical prediction model was established based on the data of 369 patients from the Department of Infectious Diseases.

PET/CT features and clinical parameters, including patient general characteristics, specific signs, blood cell counts, biochemical indexes, and immunological indicators, were included in the screening. Relevant blood indicators included not only the values measured at admission, but also the maximum and minimum values over the course of disease. Beneficial predictors that contributed to improving diagnostic efficacy were identified. For each significant independent variable, a more detailed analysis was performed (Table 4).

**Table 4** Potential diagnostic indicators and results of the logistic regression for infection, malignancy, and NIID models

Categories	Characteristics	Univariate analysis		Multivariate analysis	
		OR (95% CI)	p value	OR (95% CI)	p value
Infection	Low SUVmax of spleen, bone marrow, and lymph nodes	4.21 (2.63–6.76)	< 0.01	2.18 (1.31–3.65)	0.01
	Low SUVmax of liver ratio	2.19 (1.57–3.04)	< 0.01	2.52 (1.25–5.09)	< 0.01
	IGRA positive	6.46 (3.20–13.05)	< 0.01	13.09 (4.83–35.44)	< 0.01
	ANA and ANCA negative	13.27 (3.13–56.36)	< 0.01	20.23 (4.36–93.82)	< 0.01
	Low ESR	3.88 (2.04–7.40)	< 0.01	8.04 (3.45–18.75)	< 0.01
	High platelet	4.43 (2.10–9.37)	< 0.01	5.84 (2.10–16.23)	< 0.01
	Low neutrophilic percentage	4.06 (2.33–7.08)	< 0.01	3.62 (1.77–7.38)	< 0.01
	Low LDH	4.04 (2.61–6.27)	< 0.01	3.46 (1.83–6.53)	< 0.01
	Rash negative	2.80 (1.59–4.93)	< 0.01	2.81 (1.30–6.07)	< 0.01
Malignancy	SUVmax	1.25 (1.18–1.32)	< 0.01	1.34 (1.24–1.46)	< 0.01
	LDH /100	1.16 (1.09–1.22)	< 0.01	1.30 (1.16–1.46)	< 0.01
	Low SF	1.58 (0.82–3.04)	0.17	9.89 (2.87–34.09)	< 0.01
	High nasopharynx SUVmax	8.37 (3.07–22.77)	< 0.01	6.59 (1.59–27.29)	< 0.01
	Weight loss	4.00 (2.34–6.83)	< 0.01	6.19 (2.70–14.22)	< 0.01
	Low platelet	6.10 (3.66–10.16)	< 0.01	5.96 (2.72–13.05)	< 0.01
	Splenomegaly	6.12 (3.53–10.62)	< 0.01	3.91 (1.64–9.32)	< 0.01
	ANA or ANCA positive	12.28 (5.53–27.29)	< 0.01	64.74 (18.74–223.65)	< 0.01
NIID	Low SUVmax of liver ratio	6.55 (2.91–14.76)	< 0.01	15.32 (4.26–55.03)	< 0.01
	High platelet	3.19 (1.85–5.47)	< 0.01	9.75 (3.65–26.03)	< 0.01
	Rash positive	4.58 (2.63–7.97)	< 0.01	11.06 (4.33–28.28)	< 0.01
	High SF	4.12 (2.36–7.18)	< 0.01	7.02 (2.69–18.27)	< 0.01
	High neutrophilic percentage	4.43 (2.88–6.83)	< 0.01	6.69 (3.43–13.06)	< 0.01
	Young	2.56 (1.53–4.29)	< 0.01	3.03 (1.34–6.86)	< 0.01

NIID noninfectious inflammatory disease; OR odds ratio; CI confidence interval; ESR erythrocyte sedimentation rate; LDH lactate dehydrogenase; SF serum ferritin; SUVmax the maximum standardized uptake value; IGRA interferon gamma release assay; ANA antinuclear antibody; ANCA anti-neutrophil cytoplasm antibody



Factors with higher OR values for diagnosing infection included: low SUVmax (the “hottest” lesion, spleen, bone marrow, and lymph nodes), high platelet count, low neutrophilic percentage, low ESR, low LDH, positive IGRA, negative ANA and ANCA, and negative rash (Table 4). The probability of infection could be calculated according to the formula in Table 5. The AUC was 0.89 (95% CI 0.86–0.92) (Fig. 2). When the optimal cutoff point was 0.46, the sensitivity, specificity, positive predictive value (PPV), and negative predictive value (NPV) were 81.5%, 81.6%, 76.4%, and 85.4%, respectively.

The model for predicting malignancy included the following parameters: high SUVmax (the “hottest” lesion and nasopharynx), low platelet count, high LDH, low SF, weight loss, and splenomegaly (Table 4). The probability of malignancy could be calculated according to the formula in Table 5. The AUC was 0.94 (95% CI 0.92–0.97) (Fig. 2). When the optimal cutoff point was 0.19, the sensitivity, specificity, PPV, and NPV were 90.6%, 87.0%, 71.8%, and 94.0%, respectively.

The model for predicting NIID was composed of low SUVmax (the “hottest” lesion), high platelet count,

high neutrophilic percentage, high SF, positive ANA or ANCA, positive rash, and young age (Table 4). The probability of NIID could be calculated according to the formula in Table 5. The AUC was 0.95 (95% CI 0.93–0.97) (Fig. 2). When the optimal cutoff point was 0.21, the sensitivity, specificity, PPV, and NPV were 90.8%, 88.4%, 75.0%, and 93.5%, respectively.

**Diagnostic model validation**

A total of 155 patients from other departments comprised an independent external validation cohort. The proportion of patients in the training and validation data sets was close to 7:3, as previously described [32, 33].

According to the above models, the probabilities of the corresponding diseases in the validation cohort were calculated, and the accuracies were further analyzed (Fig. 3). In the validation cohort, the AUC of the infectious disease model was 0.88 (95% CI 0.82–0.93), and when the cutoff point was 0.46, the model sensitivity and specificity were 86.4% and 79.8%, respectively. The AUC of the malignancy model in the validation cohort was 0.93 (95% CI 0.89–0.98). When the cutoff point was 0.19, the model

**Table 5** Formulas for the Infection, malignancy, and NIID prediction model

Categories	Formula
Infection prediction model	$\text{logit}(p) = 0.92 * (\text{maximum SUVmax of spleen, bone marrow and lymph node} < 5.7 = 1) + 0.78 * (2.3 \leq \text{SUVmax of liver ratio} < 4.7 = 1, \text{SUVmax of liver ratio} < 2.3 = 2) + 1.76 * (\text{maximum platelets} > 132 * 10^9 / \text{L} = 1) + 1.29 * (\text{minimum neutrophilic percentage} < 65\% \text{ or maximum neutrophilic percentage} < 85\% = 1) + 2.09 * (\text{ESR} \leq 96 \text{ mm/H} = 1) + 1.24 * (\text{maximum LDH} \leq 340 \text{ U/L} = 1) + 2.57 * \text{IGRA} (\text{positive} = 1) + 3.01 * \text{ANA and ANCA} (\text{both negative} = 1) + 1.03 * \text{rash} (\text{negative} = 1) - 10.17$
Malignancy prediction model	$0.29 * \text{SUVmax} + 1.89 * (\text{nasopharynx SUVmax} \geq 5.6 = 1) + 1.79 * (35 * 10^9 / \text{L} < \text{platelet} \leq 170 * 10^9 / \text{L} = 1, \text{platelet} < 35 * 10^9 / \text{L} = 2) + 0.26 * \text{LDH} / 100 + 2.29 * (\text{SF} < 3200 \text{ ug/L} = 1) + 1.36 * \text{splenomegaly} (\text{splenic thickness} \geq 4.7 \text{ cm} = 1) + 1.82 * (\text{weight loss} = 1) - 8.64$
NIID prediction model	$\text{logit}(p) = 2.73 * (\text{SUVmax of liver ratio} \leq 2.8 = 1) + 2.28 * (\text{platelet} > 210 * 10^9 / \text{L} = 1) + 1.9 * (\text{maximum neutrophilic percentage} \geq 85.7\%, \text{minimum neutrophilic percentage} \geq 52.5\%, \text{both positive} = 2, \text{either positive} = 1) + 1.95 * (\text{SF} \geq 3200 \text{ ug/L} = 1) + 4.17 * \text{ANA and ANCA} (\text{either positive} = 1) + 2.4 * \text{rash} (\text{positive} = 1) + 1.11 * \text{young} (\text{age} \leq 43 \text{ years} = 1) - 9.8$

NIID noninfectious inflammatory disease; SUVmax the maximum standardized uptake value; ESR erythrocyte sedimentation rate; LDH lactate dehydrogenase; IGRA interferon gamma release assay; ANA antinuclear antibody; ANCA anti-neutrophil cytoplasm antibody; SF serum ferritin

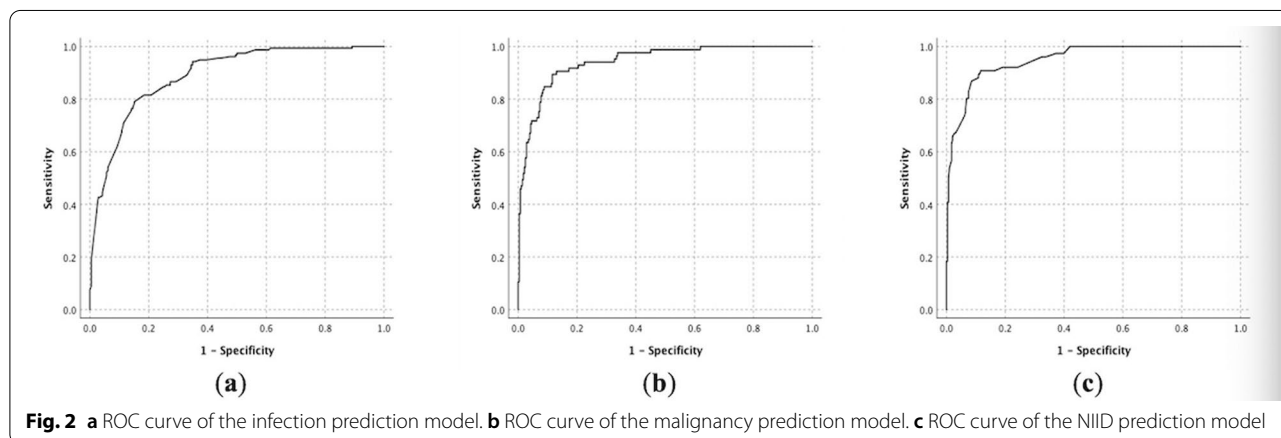
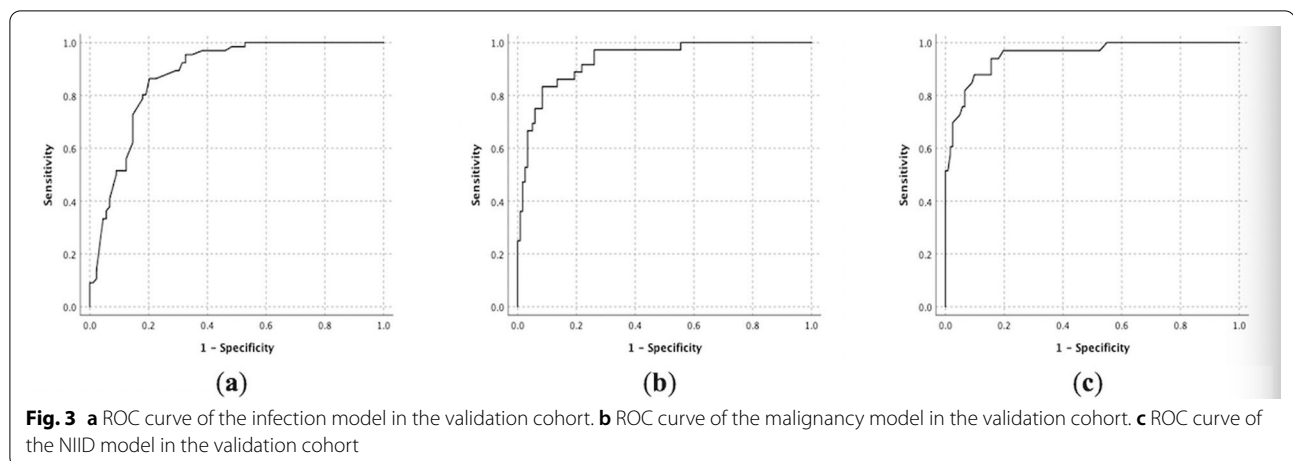


**Fig. 2** a ROC curve of the infection prediction model. b ROC curve of the malignancy prediction model. c ROC curve of the NIID prediction model



sensitivity was 86.1%, and the specificity was 85.7%. The AUC for validation of the NIID model in the cohort was 0.95 (95% CI 0.92–0.99), and when the cutoff point was 0.21, the model sensitivity was 90.9%, and the specificity was 84.4%.

## Discussion

Due to the complexity and diversity of FUO-related diseases, the multiplicity of etiologies, the atypical symptoms, and the small number of diagnostic clues, diagnosing the intrinsic etiologies of FUO remains a challenge for contemporary clinicians, requiring extensive time-consuming physical and laboratory tests and even diagnostic treatment. In this study, infection (223/524, 42.6%) accounted for the largest proportion of cases. A total of 23.1% (121/524) of patients had malignancies, 20.8% (109/524) had NIIDs, and 9.4% (49/524) received no diagnosis. This etiological distribution is in concordance with a Chinese survey involving 1641 patients with FUO [34]. Early identification of the underlying cause and implementation of appropriate empirical treatment are effective strategies for patients with FUO.

The high sensitivity and wide visual field of PET/CT are helpful in detecting lesions that are clinically unknown or undetectable with conventional imaging techniques and in obtaining multisystem observations [25, 26]. FDG uptake is an indicator of increased intracellular glucose metabolism, and this molecule can be absorbed not only by malignant cells, but also by cells involved in infection and inflammation [13, 14, 18, 19, 25]. The presence of abnormal uptake can help guide further investigations, leading to a definitive diagnosis. The absence of abnormal absorption reasonably ensures that the possible underlying conditions are not present, thus avoiding unnecessary additional testing. Therefore, in recent years, the diagnostic role of PET/

CT in FUO has been widely recognized, especially in oncology [11–19]. SUVmax can be obtained by routine scanning, which is easy to obtain and reproduce and directly reflects the highest activity of the lesion, so it is widely used in clinical practice. Consistent with previous studies, the uptake of FDG in neoplastic diseases was significantly higher than that in other diseases. SUVmax had moderate diagnostic performance for malignancy with an AUC of 0.79 and a low diagnostic performance for nonneoplastic diseases, which is not satisfactory for clinicians. Although the lymph nodes and bone marrow were the most common sites of the highest enhancement in all etiologies, other hyperenhancement sites varied among etiologies. In particular, nasopharyngeal hypermetabolism was common in tumors; the final diagnostic model confirmed that nasopharyngeal metabolic characteristics were helpful for the diagnosis of tumors.

Previous studies divided positive PET/CT results into focal FDG uptake and nonspecific abnormal uptake (NAU). NAU manifests as spleen and bone marrow diffuse high uptake and multiple reactive hyperplasia lymph nodes with high uptake and symmetrical distribution. NAU is common and has been considered a negative or a minor factor in diagnosis in some studies [12–15, 17, 18]. However, there were significant differences in the metabolic characteristics of the spleen, bone marrow, and lymph nodes among different etiologies of FUO. In general, infection manifested a low incidence of increased FDG uptake and a low corresponding SUVmax, malignancy was characterized by a high incidence of increased FDG avidity and a high corresponding SUVmax, and NIID showed a high incidence of increased FDG uptake (except in the central lymph nodes) but a low corresponding SUVmax. Nevertheless, these parameters performed finitely when

used separately in differentiating the cause of FOU into infection, malignancy, and NIID, and their diagnostic efficiency need to be further improved.

Preliminary studies have demonstrated that clinical parameters, such as rash, weight loss, SF, and LDH, can be combined with imaging findings to obtain a more confident diagnosis [15, 35]. Some researchers have built diagnostic models for patients with FOU, but only for particular causes or patients [9, 10, 15]. Efstathiou et al. focused on the distinction between infectious and non-infectious, and XU et al. emphasized the discrimination of bacterial infections. Wang's research was also based on PET/CT and clinical features, but the diagnostic formula was mainly aimed at NAU patients, which was not simple and feasible in practice. Unlike previous studies that focused only on blood markers at admission, this study suggested that dynamic changes in these parameters were more conducive to a differential diagnosis, further confirming the importance of dynamic observation in the diagnosis of FOU. The indexes used to construct the models were consistent with the clinical characteristics of the corresponding diseases. There are some common clinical indicators used to identify certain etiology, such as IGRA for infection, low platelet count and splenomegaly for cancer, rash, ANA and ANCA for NIID, but they are not sufficiently sensitive and specific when used alone. Theoretically, the combined application can further improve the diagnostic performance, but there is no consensus on how to combine them. Through a large sample population in the real world, the favorable factors conducive to the etiological classification of FOU were screened out, and the weight of each index was further analyzed to obtain the formula. The AUCs of the infection, malignancy, and NIID diagnostic models were 0.89, 0.94, and 0.95, respectively, showing good discrimination ability. Similar results were obtained for the validation cohort, which verified the stability of the models. Especially for infectious diseases and NIID, the diagnostic model combined with other clinical indicators significantly improves the diagnostic efficacy of PET/CT. When PET/CT cannot provide a clear etiological diagnosis, the diagnostic models can be used to calculate the probability of each classification, rapidly and accurately distinguishing the etiologies of FOU: infectious or non-infectious, malignant or nonmalignant, and typical NIID or non-NIID.

The strengths of our study include its prospective setting, the large sample size divided into prediction and validation cohorts, the combination of clinical parameters and PET/CT imaging, and the creation of diagnostic models in a real-life clinical setting. The models were established according to PET/CT characteristics, which further improved the diagnostic efficiency of this imaging

modality in FOU. The models performed satisfactorily in differentiating FOU cases, especially for malignancy and NIID. When the etiology of FOU is unclear or the clinical features are not obvious, the models can help clinicians achieve a more accurate FOU diagnosis, avoid unnecessary invasive procedures and unreasonable use of antibiotics, and reduce the rate of missed diagnosis and delayed diagnosis.

There are some limitations to this study. The single-center design likely limits the robustness of our findings. Multicenter and larger sample studies are needed to further confirm these results. Due to the wide variety of infectious diseases and obvious differences among subgroups, the sensitivity and specificity of the infection model are not adequately high. In later stages, we will further subdivide the types of infectious diseases and build more sophisticated diagnostic models. Since SUVmax is closely related to acquisition time, PET scanner, and patient metabolism and may represent only a small pixel, the use of SUVmax in this study may have limitations. More metabolic indicators, such as SUVmean or SUVpeack, can be considered in the later stage.

## Conclusions

<sup>18</sup>F-FDG PET/CT has a certain level of sensitivity and accuracy in the diagnosis of FOU, which can be further improved by combining clinical parameters. Diagnostic models based on PET/CT show excellent performance in the diagnosis of FOU and can be used as a reliable tool to discriminate the cause of the condition. According to the current study results on FOU patients, it is important to further investigate the application of PET/CT in diagnosing nonneoplastic diseases.

## Abbreviations

FOU: Fever of unknown origin; <sup>18</sup>F-FDG PET/CT: <sup>18</sup>F-fluorodeoxyglucose positron emission tomography/computed tomography; NIID: Noninfectious inflammatory disease; AUC: Area under the receiver operating characteristic curve; PDCs: Potential diagnostic clues; ESR: Erythrocyte sedimentation rate; LDH: Lactate dehydrogenase; SF: Serum ferritin; IGRA: Interferon gamma release assay; SUVmax: The maximum standardized uptake value; IQR: Interquartile range; OR: Odds ratio; CI: Confidence interval; ANA: Antinuclear antibody; ANCA: Anti-neutrophil cytoplasm antibody; NAU: Nonspecific abnormal uptake; LN: Lymph node.

## Supplementary Information

The online version contains supplementary material available at <https://doi.org/10.1186/s13550-022-00937-4>.

**Additional file1. Fig. S1.** The ROC curve of PET/CT characteristics in diagnosing infection, malignancy, and NIID. **Table S1.** Clinical diagnosis and etiological classification in 524 patients with FOU. **Table S2.** Lesions with the most intense FDG uptake for 477 patients with FOU.



**Acknowledgements**

The authors thank all the study participants.

**Author contributions**

Conception and design were done by all authors; acquisition of data was done by JC, NNX, and WCZ; analysis and interpretation of data was carried out by JC, MYX, DX, QRR, and JXS; statistical analysis was carried out by JC; drafting the article or revising it critically for important intellectual content was done by all authors. All authors read and approved the final manuscript.

**Funding**

This research received no external funding.

**Availability of data and materials**

The datasets generated and/or analyzed during the current study are not publicly available due to data security restrictions but are available from the corresponding author on reasonable request.

**Declarations****Ethics approval and consent to participate**

All methods were carried out in accordance with the ethical standards as laid down in the 1964 Declaration of Helsinki and its later amendments. The research protocol was reviewed and approved by the Huazhong University of Science and Technology Clinical Trial Ethics Committee ([2014] EC-No. 16). Written informed consent was obtained from all participants.

**Consent for publication**

Not applicable.

**Competing interests**

The authors declare that they have no competing interests.

**Author details**

<sup>1</sup>Department of Infectious Diseases, Tongji Hospital, Tongji Medical College, Huazhong University of Science and Technology, 1095 Jiefang Avenue, Wuhan 430030, China. <sup>2</sup>Institute of Pathology, Tongji Hospital, Tongji Medical College, Huazhong University of Science and Technology, 1095 Jiefang Avenue, Wuhan 430030, China.

Received: 11 August 2022 Accepted: 24 September 2022

Published online: 28 October 2022

**References**

- Petersdorf RG, Beeson PB. Fever of unexplained origin: report on 100 cases. *Medicine*. 1961;40:1–30.
- Petersdorf RG. Fever of unknown origin. An old friend revisited. *Arch Intern Med*. 1992;152(1):21–2.
- Durack DT, Street AC. Fever of unknown origin—reexamined and redefined. *Curr Clin Top Infect Dis*. 1991;1:35–51.
- Wright WF, Auwaerter PG. Fever and fever of unknown origin: review, recent advances, and lingering dogma. *Open Forum Infect Dis*. 2020;7(5):ofaa132. <https://doi.org/10.1093/ofid/ofaa132>.
- Cunha BA, Lortholary O, Cunha CB. Fever of unknown origin: a clinical approach. *Am J Med*. 2015;128(10):1138.e1–1138.e15. <https://doi.org/10.1016/j.amjmed.2015.06.001>.
- Haidar G, Singh N. Fever of unknown origin. *N Engl J Med*. 2022;386(5):463–77. <https://doi.org/10.1056/NEJMra2111003>.
- Knockaert DC, Vanderschueren S, Blockmans D. Fever of unknown origin in adults: 40 years on. *J Intern Med*. 2003;253(3):263–75. <https://doi.org/10.1046/j.1365-2796.2003.01120.x>.
- Yan YJ, Chen CY, Liu YY, et al. Application of machine learning for the prediction of etiological types of classic fever of unknown origin. *Front Public Health*. 2021;9: 800549. <https://doi.org/10.3389/fpubh.2021.800549>.
- Xu T, Wang L, Wu S, et al. Utility of a simple scoring system in differentiating bacterial infections in cases of fever of unknown origin. *Clin Infect Dis*. 2020;71(Suppl 4):S409–15. <https://doi.org/10.1093/cid/ciaa1520>.
- Efstathiou SP, Pefanis AV, Tsiakou AG, et al. Fever of unknown origin: discrimination between infectious and non-infectious causes. *Eur J Intern Med*. 2010;21(2):137–43. <https://doi.org/10.1016/j.ejim.2009.11.006>.
- Letertre S, Fesler P, Zerkowski L, et al. Place of the 18F-FDG-PET/CT in the diagnostic workup in patients with classical fever of unknown origin (FUO). *J Clin Med*. 2021;10(17):3831. <https://doi.org/10.3390/jcm10173831>.
- Ergül N, Halac M, Cermik TF, et al. The diagnostic role of FDG PET/CT in patients with fever of unknown origin. *Mol Imaging Radionucl Ther*. 2011;20(1):19–25. <https://doi.org/10.4274/MIRT.20.04>.
- Tokmak H, Ergonul O, Demirkol O, Cetiner M, Ferhanoglu B. Diagnostic contribution of (18)F-FDG-PET/CT in fever of unknown origin. *Int J Infect Dis*. 2014;19:53–8. <https://doi.org/10.1016/j.ijid.2013.10.009>.
- Wang Q, Li YM, Li Y, et al. 18F-FDG PET/CT in fever of unknown origin and inflammation of unknown origin: a Chinese multi-center study. *Eur J Nucl Med Mol Imaging*. 2019;46(1):159–65. <https://doi.org/10.1007/s00259-018-4121-1>.
- Wang WX, Cheng ZT, Zhu JL, et al. Combined clinical parameters improve the diagnostic efficacy of 18F-FDG PET/CT in patients with fever of unknown origin (FUO) and inflammation of unknown origin (IUO): a prospective study in China. *Int J Infect Dis*. 2020;93:77–83. <https://doi.org/10.1016/j.ijid.2020.01.030>.
- Hung BT, Wang PW, Su YJ, et al. The efficacy of 18F-FDG PET/CT and 67Ga SPECT/CT in diagnosing fever of unknown origin. *Int J Infect Dis*. 2017;62:10–7. <https://doi.org/10.1016/j.ijid.2017.06.019>.
- Gafter-Gvili A, Raibman S, Grossman A, et al. [18F] FDG-PET/CT for the diagnosis of patients with fever of unknown origin. *Q J Med*. 2015;108(4):289–98. <https://doi.org/10.1093/qjmed/hcu193>.
- Schönau V, Vogel K, Englbrecht M, et al. The value of 18F-FDG-PET/CT in identifying the cause of fever of unknown origin (FUO) and inflammation of unknown origin (IUO): data from a prospective study. *Ann Rheum Dis*. 2018;77(1):70–7. <https://doi.org/10.1136/annrheumdis-2017-211687>.
- Georga S, Exadaktylou P, Petrou I, et al. Diagnostic value of 18F-FDG-PET/CT in patients with FUO. *J Clin Med*. 2020;9(7):2112. <https://doi.org/10.3390/jcm9072112>.
- Bleeker-Rovers CP, Vos FJ, Mudde AH, et al. A prospective multicenter study of the value of FDG-PET as part of a structured diagnostic protocol in patients with fever of unknown origin. *Eur J Nucl Med Mol Imaging*. 2007;34(5):694–703. <https://doi.org/10.1007/s00259-006-0295-z>.
- Pereira AM, Husmann L, Sah BR, et al. Determinants of diagnostic performance of 18F-FDG PET/CT in patients with fever of unknown origin. *Nucl Med Commun*. 2016;37(1):57–65. <https://doi.org/10.1097/MNM.0000000000000395>.
- Jamar F, Buscombe J, Chiti A, et al. EANM/SNMMI guideline for 18F-FDG use in inflammation and infection. *J Nucl Med*. 2013;54(4):647–58. <https://doi.org/10.2967/jnumed.112.112524>.
- Hess S, Hansson SH, Pedersen KT, et al. FDG-PET/CT in infectious and inflammatory diseases. *PET Clin*. 2014;9(4):497–519. <https://doi.org/10.1016/j.cpet.2014.07.002>.
- Vaidyanathan S, Patel CN, Scarsbrook AF, et al. FDG PET/CT in infection and inflammation—current and emerging clinical applications. *Clin Radiol*. 2015;70(7):787–800. <https://doi.org/10.1016/j.crad.2015.03.010>.
- Kouijzer JJE, Mulders-Manders CM, Bleeker-Rovers CP, et al. Fever of unknown origin: the value of FDG-PET/CT. *Semin Nucl Med*. 2018;48(2):100–7. <https://doi.org/10.1053/j.semnuclmed.2017.11.004>.
- Besson FL, Chaumet-Riffaud P, Playe M, et al. Contribution of 18F-FDG PET in the diagnostic assessment of fever of unknown origin (FUO): a stratification-based meta-analysis. *Eur J Nucl Med Mol Imaging*. 2016;43(10):1887–95. <https://doi.org/10.1007/s00259-016-3377-6>.
- Sioka C, Assimakopoulos A, Fotopoulos A. The diagnostic role of (18)F fluorodeoxyglucose positron emission tomography in patients with fever of unknown origin. *Eur J Clin Invest*. 2015;45(6):601–8. <https://doi.org/10.1111/eci.12439>.
- Takeuchi M, Dahabreh IJ, Nishihashi T, et al. Nuclear imaging for classic fever of unknown origin: meta-analysis. *J Nucl Med*. 2016;57(12):1913–9. <https://doi.org/10.2967/jnumed.116.174391>.
- Wright WF, Auwaerter PG, Dibble EH, et al. Imaging a fever—redefining the role of 2-deoxy-2-[18F] fluoro-D-glucose-positron emission tomography/computed tomography in fever of unknown origin investigations. *Clin Infect Dis*. 2021;72(7):1279–86. <https://doi.org/10.1093/cid/ciaa1220>.

30. Wu ZH, Xing MY, Wei S, et al. Establishment of a predictive model related to pathogen invasion for infectious diseases and its diagnostic value in fever of unknown origin. *Curr Med Sci.* 2018;38(6):1025–31. <https://doi.org/10.1007/s11596-018-1979-x>.
31. Chinese Society of Nuclear Medicine (2014) Basic requirements of clinical quality control and quality assurance on SPECT(/CT) and PET/ CT (2014 edition). *Chin J Nucl Med Mol Imaging.* 2014;8(6):343–448. **(Chinese)**
32. Hu TD, Wang SP, Huang L, et al. A clinical-radiomics nomogram for the preoperative prediction of lung metastasis in colorectal cancer patients with indeterminate pulmonary nodules. *Eur Radiol.* 2019;29(1):439–49. <https://doi.org/10.1007/s00330-018-5539-3>.
33. Chen XF, Tang YY, Mo YK, et al. A diagnostic model for coronavirus disease 2019(COVID-19) based on radiological semantic and clinical features: a multi-center study. *Eur Radiol.* 2020;30(9):4893–902. <https://doi.org/10.1007/s00330-020-06829-2>.
34. Zhou GY, Zhou Y, Zhong CJ, et al. Retrospective analysis of 1,641 cases of classic fever of unknown origin. *Ann Transl Med.* 2020;8(11):690. <https://doi.org/10.21037/atm-20-3875>.
35. Zhao MZ, Ruan QR, Xing MY, et al. A diagnostic tool for identification of etiologies of fever of unknown origin in adult patients. *Curr Med Sci.* 2019;39(4):589–96. <https://doi.org/10.1007/s11596-019-2078-3>.

### Publisher's Note

Springer Nature remains neutral with regard to jurisdictional claims in published maps and institutional affiliations.

**Submit your manuscript to a SpringerOpen<sup>®</sup> journal and benefit from:**

- ▶ Convenient online submission
- ▶ Rigorous peer review
- ▶ Open access: articles freely available online
- ▶ High visibility within the field
- ▶ Retaining the copyright to your article

---

Submit your next manuscript at ▶ [springeropen.com](https://www.springeropen.com)

---